Synthesis of Wideband WAIMs within the System-by-Design Framework

G. Oliveri, M. Salucci, N. Anselmi, and A. Massa

Abstract

In this work, the design of wideband wide-angle impedance matching (*WAIM*) structures is proposed for waveguide-fed planar phased arrays. An innovative System-by-Design (*SbD*) approach is exploited to determine the geometrical descriptors of the WAIM, which is composed by a metasurface of regularly-arranged microstrip printed unit cells. The proposed solution technique is based on the combination of elementary functional blocks aimed at (i) exploring the search space, (ii) analyzing the resulting metasurface structure to deduce the equivalent permittivity/permeability tensors, (iii) computing the phased array response, and (iv) linking the obtained result with the problem constraints and objectives to determine the associated cost function. Some numerical results are shown in order to assess the effectiveness of the *SbD*-based design strategy.

1 Introduction on FSS

A Frequency Selective Surface (FSS) is a periodic surface whose response to incident radiation varies with frequency. It can reflect, transmit, or absorb different amounts of radiation at different frequencies.

Regarding the Bandwidth, the larger the interelement space is, the narrower the bandwidth and vice versa. The FSS could be divided into at least 4 groups:

1. The center connected or N-poles, such as the simple straight element, three-legged element, the jerusalem cross and the square spiral.
2. The loop types such as the three- and four-legged loaded elements; the circular loops; and the square and hexagonal loops.
3. Solid interior or plate types of various shapes.
4. Combinations.

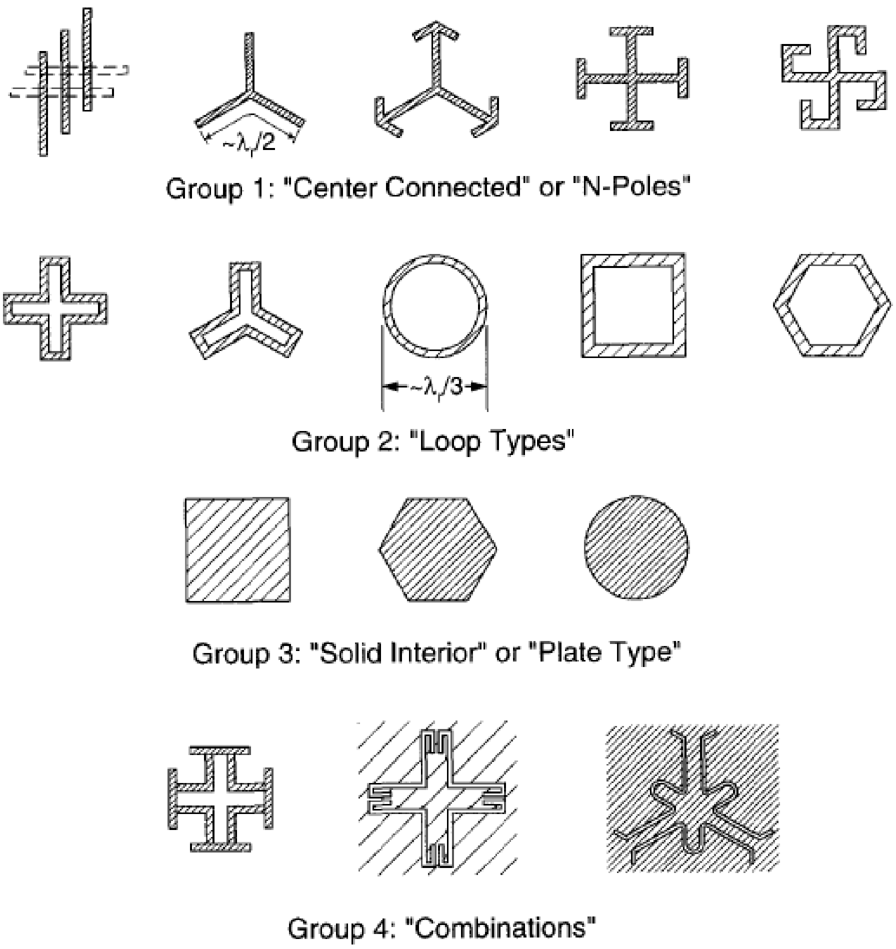

Figure 1: Examples of FSS

Some figures will be describe deeply in the following paragraphs:

Unloaded Tripole Array:

The unloaded tripole consists of 3 simple straight dipoles all connected to a same point.

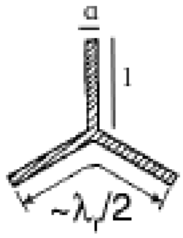

Figure 2: Unloaded Tripole Array

This shape, thanks to the thin arms, has the capability to pack itself very close to each other.

This characteristics to be packed tightly, making the interelement spacings smaller, lead to have a larger bandwidth respect to the 4-legged case.

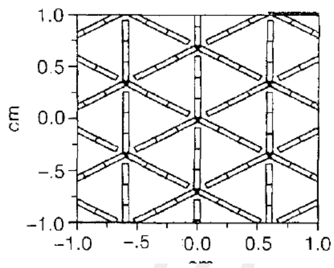

Figure 3: Replicated Unloaded Tripole Array

Anchor Elements:

This shape is a simple modification of the unloaded tripole leading to increased bandwidth. It is created only adding to the end of each "arm" a capacitive load. It naturally leads to smaller elements resulting in a significantly smaller inter-element spacing.

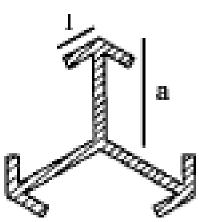

Figure 4: Anchor Elements

Jerusalem Cross:

Basically it consists of a pair of crossed dipoles with end loading.

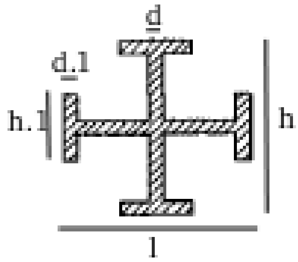

Figure 5: Jerusalem Cross

Simple 5 Crosses (all indipendent arms):

The idea is to make each arm's dimension indipendent in order to better optimize the resulting optimal shape.

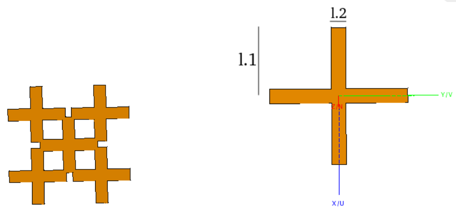

a) b)

Figure 6: a) 5 Crosses, b) detail

Four-legged Loaded Element :

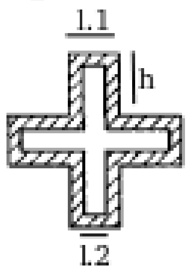

Figure 7: Four-legged Loaded Element

If a large bandwidth is desired, it will in general be advantageous to go to a loop element with a large opening.

All FSSs can change bandwidth by variation of the inter-element spacings, in particular the four-legged and three-legged elements are capable of considerable variation by changing the elements themselves.

Three-legged Loaded Element:

The geometry derives from the four-legged loaded element. In particular these elements resonate when their circumferences are approximately one full wavelength, and they show a load null at the frequency where the legs are approximately $\frac{\lambda}{4}$ long.

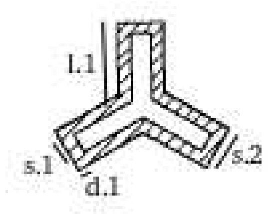

Figure 8: Three-legged Loaded Element

As regard the bandwidth, it is considerably more broadbanded than the four-legged cases , the primary reason being that the inter-element spacings are considerably smaller;

In other words, **the bigger the inter-element space is, the lower the bandwidth**.

Circle Loop:

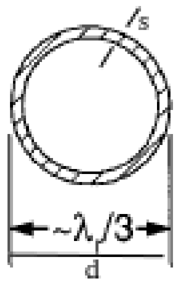

Figure 9: Circle Shape

1.1 Resume:

	Control Parameter	Operative Freq
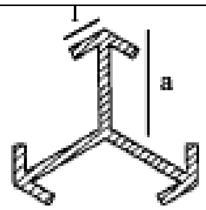	l: sub-arm length; a: arm length; + each arm indipendent	λ dependent
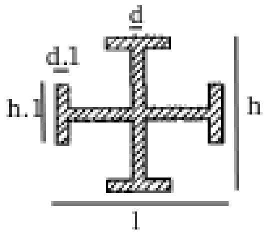	h,l and d: cross dimensions; d.1,h.1:capacitive load dimensions + each load indipendent	λ dependent
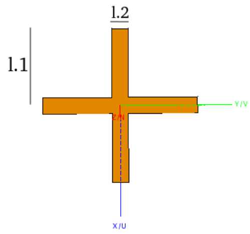	l1: arm 1 length; l2: arm 1 width; + each arm is indipendent	λ dependent
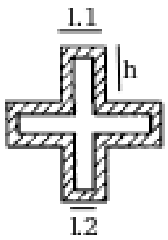	s1, s1: inner and outer length; h: arm 1 heigth + each arm indipendent	λ dependent
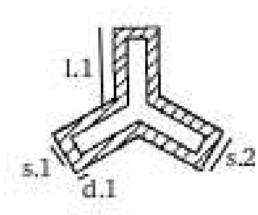	l1: length of arm 1; d1: thickness s1, s1: inner and outer width + each arm could be indipendent	λ dependent BW larger than 4-legged
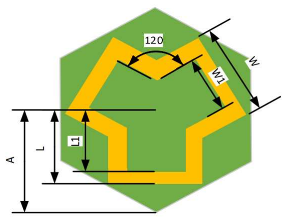	A, L, L1, W, W1 possibility to set each arm independenty angle between arms: 120°	λ dependent
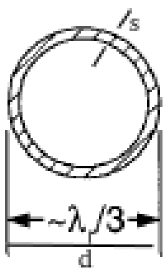	s: thickness of the patch d: diametre;	λ dependent $\frac{\lambda}{4}$

Table 1: Resume

2 Implementazione Wideband:

2.1 Simulazioni effettuate con $f \in [14.25; 16.25]\ GHz$

l modello usato è formato dalle 5 croci semplici delle quali è possibile modificare lunghezza e larghezza delle braccia e angolo di tilt. Queste sono appunto le 3 incognite che andrà a modificare il PSO:

- $CrossLength$
- $CrossWidth$
- $TiltAngle$

Nel processo di omogenizzazione viene utilizzata una distanza di $d = 1.05e^{-3}\lambda$ tra WAIM e l'array di guide d'onda. Il layer di materiale dielettrico omogeneo simulato dal MbD avrà poi uno spessore $d' = 2.1e^{-3}\lambda$.

Nel caso Wideband, viene effettuata una simulazione per ogni frequenza utilizzatata

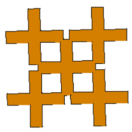

Figure 10: Croce, modello FEKO

Parametri PSO:

- swarm_size=10;
- max_iteration_number=20;
- ftol=0.0001;
- unknown_number=3

  Parametri da ottimizzare:

  - $CrossLength = [0.0012 - 0.00135]$
  - $CrossWidth = [0.00002 - 0.001]$
  - $TiltAngle = [0° - 3°]$
- swarm_filename=Initial.Swarm
- saving_percentage=100;
- inertial_weigth=0.4;
- inertial=2 (consider constant inertial velocity)

- choose_parameter_ab=1 (a≠b Random)
- $\alpha = \beta = 0.4$
- $c1 = c2 = 2.0$

Fitness:

$$\Psi = \frac{1}{183} \cdot \sum_{\phi=0,45,90} \sum_{\theta=0}^{60} 1 - \Gamma^2$$

La Fitness è stata calcolata minimizzando il coefficiente di Riflessione sui 3 piani: E-plane ($\phi = 0$), D-plane ($\phi = 45$) e H-plane ($\phi = 90$) considerando l'angolo θ da 0 a 60°

- $\theta = [0 : 60]$
- $\phi = [0; 45; 90]$

$\Psi_{min} = 5.80888 \cdot 10^{-2}$

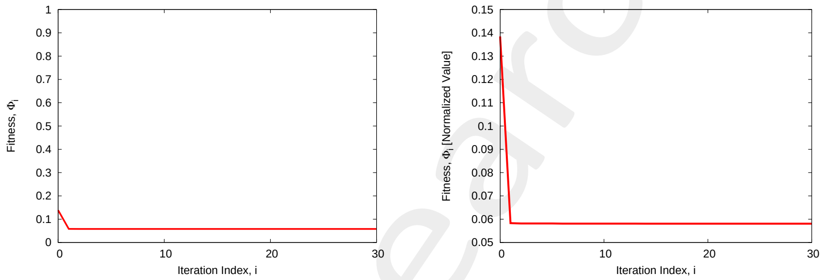

a) b)

Figure 11: a) Fitness , b) zoom

Il risultato ottimo si ottiene all'iterazione 14 particella 4:

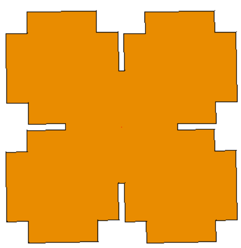

Figure 12: Unit cell, modello FEKO, figura ottima

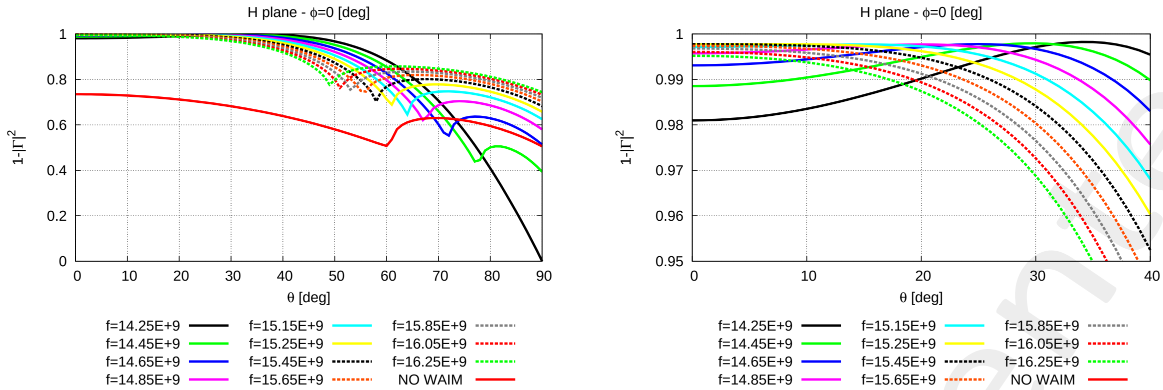

a) b)

Figure 13: a) Coefficiente di Trasmissione: Piano Phi.0 , b) zoom

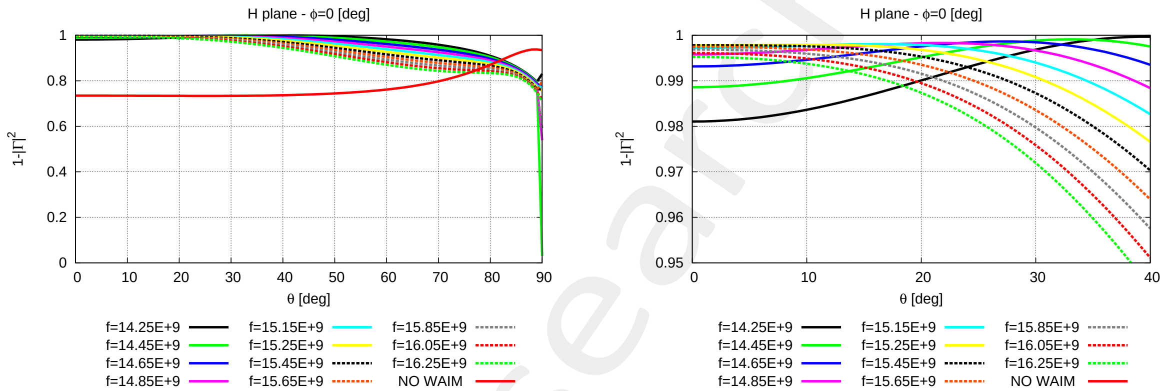

a) b)

Figure 14: a) Coefficiente di Trasmissione: Piano Phi.45 , b) zoom

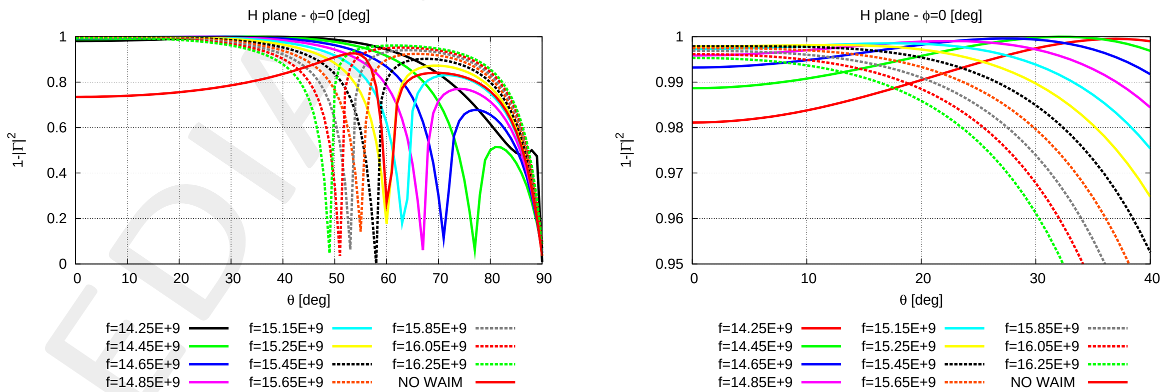

a) b)

Figure 15: a) Coefficiente di Trasmissione: Piano Phi.90 , b) zoom

2.2 Simulazioni effettuate con $f \in [14.25; 17.25]\ GHz$

$\Psi_{min} = 3.8311 \cdot 10^{-2}$

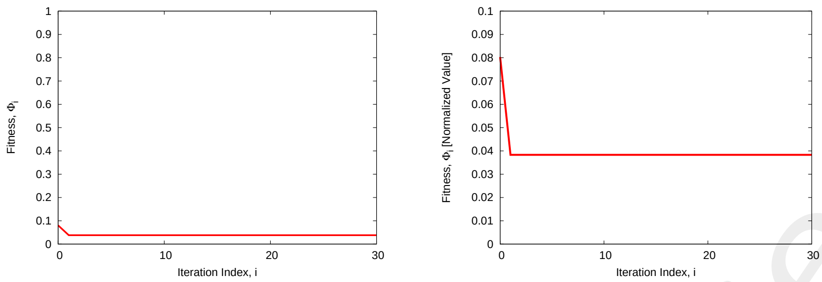

a) b)

Figure 16: a) Fitness , b) zoom

Il risultato ottimo si ottiene all'iterazione 1 particella 1:

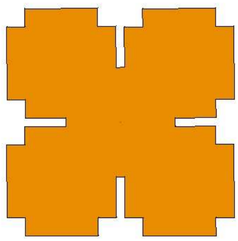

Figure 17: Unit cell, modello FEKO, figura ottima

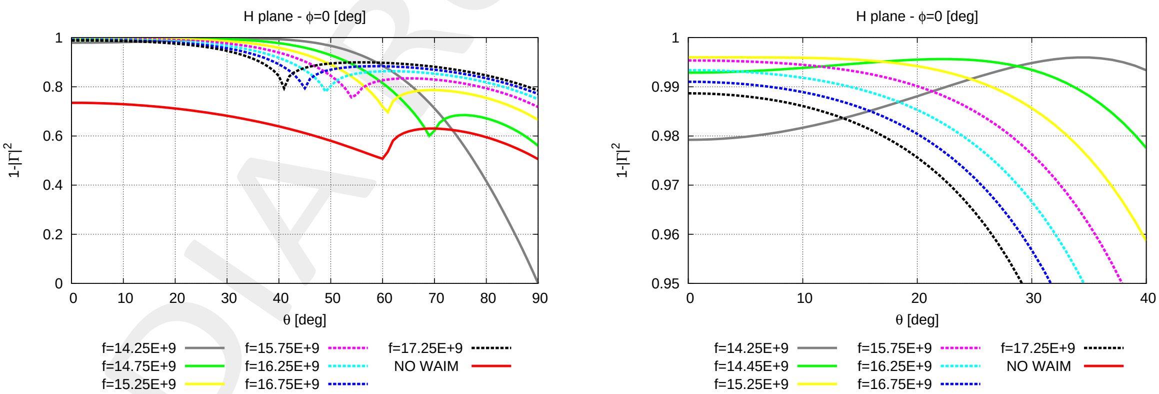

a) b)

Figure 18: a) Coefficiente di Trasmissione: Piano Phi.0 , b) zoom

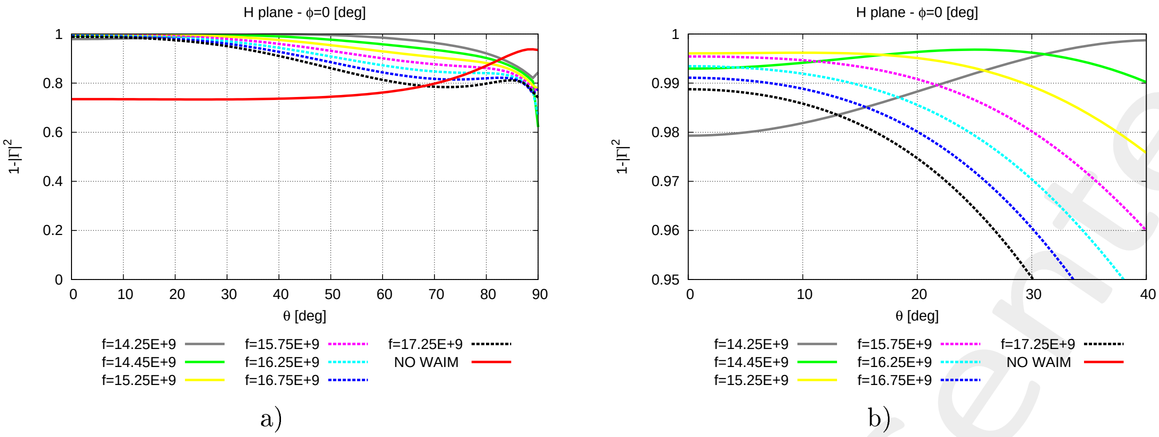

Figure 19: a) Coefficiente di Trasmissione: Piano Phi.45 , b) zoom

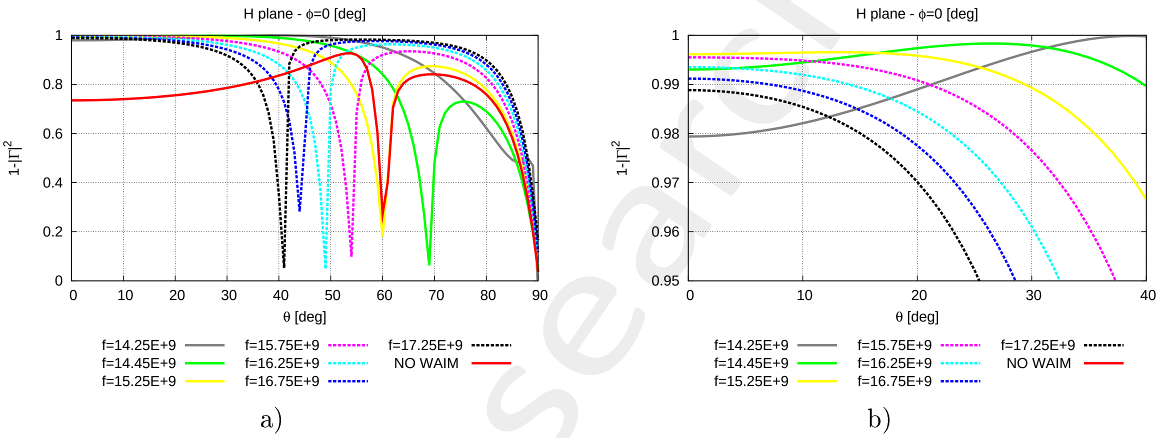

Figure 20: a) Coefficiente di Trasmissione: Piano Phi.90 , b) zoom

References

[1] G. Oliveri, M. Salucci, N. Anselmi and A. Massa, "Multiscale System-by-Design synthesis of printed WAIMs for waveguide array enhancement," *IEEE J. Multiscale Multiphysics Computat. Techn.*, vol. 2, pp. 84-96, 2017.

[2] A. Massa and G. Oliveri, "Metamaterial-by-Design: Theory, methods, and applications to communications and sensing - Editorial," *EPJ Applied Metamaterials*, vol. 3, no. E1, pp. 1-3, 2016.

[3] G. Oliveri, F. Viani, N. Anselmi, and A. Massa, "Synthesis of multi-layer WAIM coatings for planar phased arrays within the system-by-design framework," *IEEE Trans. Antennas Propag.*, vol. 63, no. 6, pp. 2482-2496, June 2015.

[4] G. Oliveri, L. Tenuti, E. Bekele, M. Carlin, and A. Massa, "An SbD-QCTO approach to the synthesis of isotropic metamaterial lenses," *IEEE Antennas Wireless Propag. Lett.*, vol. 13, pp. 1783-1786, 2014.

[5] A. Massa, G. Oliveri, P. Rocca, and F. Viani, "System-by-Design: a new paradigm for handling design complexity," *8th European Conference on Antennas Propag.* (EuCAP 2014), The Hague, The Netherlands, pp. 1180-1183, Apr. 6-11, 2014.

[6] G. Oliveri, E. T. Bekele, M. Salucci, and A. Massa, "Transformation electromagnetics miniaturization of sectoral and conical horn antennas," *IEEE Trans. Antennas Propag.*, vol. 64, no. 4, pp. 1508-1513, April 2016.

[7] G. Oliveri, E. T. Bekele, M. Salucci, and A. Massa, "Array miniaturization through QCTO-SI metamaterial radomes," *IEEE Trans. Antennas Propag.*, vol. 63, no. 8, pp. 3465-3476, Aug. 2015.

[8] P. Rocca, M. Benedetti, M. Donelli, D. Franceschini, and A. Massa, "Evolutionary optimization as applied to inverse problems," *Inverse Problems*, vol. 25, pp. 1-41, Dec. 2009.

[9] N. Anselmi, P. Rocca, M. Salucci, and A. Massa, "Optimization of excitation tolerances for robust beamforming in linear arrays," *IET Microwaves, Antennas & Propagation*, vol. 10, no. 2, pp. 208-214, 2016.

[10] T. Moriyama, F. Viani, M. Salucci, F. Robol, and E. Giarola, "Planar multiband antenna for 3G/4G advanced wireless services," *IEICE Electronics Express*, vol. 11, no. 17, pp. 1-10, Sep. 2014.

[11] F. Viani, "Dual-band sierpinski pre-fractal antenna for 2.4GHz-WLAN and 800MHz-LTE wireless devices," *Progress In Electromagnetics Research C*, vol. 35, pp. 63-71, 2013.

[12] F. Viani, M. Salucci, F. Robol, and A. Massa, "Multiband fractal Zigbee/WLAN antenna for ubiquitous wireless environments," *Journal of Electromagnetic Waves and Applications*, vol. 26, no. 11-12, pp. 1554-1562. 2012.

[13] F. Viani, M. Salucci, F. Robol, G. Oliveri, and A. Massa, "Design of a UHF RFID/GPS fractal antenna for logistics management," *Journal of Electromagnetic Waves and Applications*, vol. 26, pp. 480-492, 2012.

[14] P. Rocca, G. Oliveri, R. J. Mailloux, and A. Massa, "Unconventional phased array architectures and design methodologies - A review," *Proceedings of the IEEE - Special Issue on 'Phased Array Technologies'*, vol. 104, no. 3, pp. 544-560, March 2016.

[15] F. Viani, F. Robol, M. Salucci, and R. Azaro, "Automatic EMI filter design through particle swarm optimization," *IEEE Transactions on Electromagnetic Compatibility*, vol. 59, no. 4, pp. 1079-1094, Aug. 2017.